MHD Viscous Flow and Heat Transfer Induced by a Permeable Shrinking Sheet with Prescribed Surface Heat Flux

FADZILAH MD ALI[1], ROSLINDA NAZAR[2], NORIHAN MD ARIFIN[1]
[1]Department of Mathematics and Institute for Mathematical Research
Universiti Putra Malaysia
43400 UPM Serdang, Selangor
MALAYSIA

[2]School of Mathematical Sciences, Faculty of Science & Technology
Universiti Kebangsaan Malaysia,
43600 UKM Bangi, Selangor,
MALAYSIA

fadzilah@math.upm.edu.my, rmn72my@yahoo.com, norihan@math.upm.edu.my

Abstract: - The problem of magnetohydrodynamic (MHD) boundary layer flow and heat transfer due to a permeable shrinking sheet with prescribed surface heat flux is studied. The viscous fluid is electrically conducting in the presence of a uniform applied magnetic field and the induced magnetic field is neglected. The transformed nonlinear ordinary differential equations are solved numerically via the implicit finite-difference scheme known as the Keller-box method. Both two-dimensional and axisymmetric cases are considered. The results for the skin friction coefficient and the wall temperature, as well as the velocity and temperature profiles are presented and discussed for various parameters. Dual solutions exist for certain range of the suction parameter and Hartmann number. It is found that the boundary layer separation is delayed with Hartmann number.

Key-Words: - Boundary layer, Heat transfer, Magnetohydrodynamic, Shrinking sheet, Suction, Surface heat flux.

1 Introduction

The classical problem was introduced by Blasius [1] where he considered the boundary layer flow on a fixed flat plate. Different from Blasius [1], the boundary layer flow over a stretching sheet was first studied by Sakiadis [2]. Later, Crane [3] extended this idea for the two-dimensional problem where the velocity is proportional to the distance from the plate. The heat and mass transfer over a stretching sheet subject to suction or blowing (injection) was investigated by Gupta and Gupta [4] and Magyari and Keller [5]. In porous medium, Cheng [6] solved the problem of mixed convection along a vertical surface in the presence of a transverse magnetic field using integral methods. Later, Al-Azab [7] studied the mixed convection flow of an incompressible fluid past an infinite vertical porous plate with thermophoresis effect. Boricic et al. [8] considered unsteady two-dimensional MHD boundary layer with temperature gradient along the surface, while Narahari [9] gave an exact solution of the problem of an unsteady Couette flow of a viscous, incompressible fluid between two parallel plates in the presence of constant heat flux and thermal radiation.

Merkin and Mahmood [10] studied similarity solution in mixed convection boundary layer with prescribed surface heat flux, while Ramachandran et al. [11] considered two-dimensional stagnation flows adjacent to a vertical heated surface with both prescribed wall temperature and prescribed wall heat flux. Later, the problem of mixed convection flow and heat transfer along a vertical cylinder with prescribed surface heat flux was investigated by Ishak [12]. Very recently, Bachok and Ishak [13] reported the effects of suction and injection on a moving flat plate in a parallel stream with prescribed surface heat flux.

Boundary layer flow over a shrinking sheet with a power-law velocity was studied by Fang [14], while stagnation flow towards a shrinking sheet has been considered by Wang [15] and Rahimpour et al. [16]. Recently, Fang et al. [17] and Ali et al. [18] solved the problem of viscous flow induced by a shrinking sheet with time dependent deceleration taken into account and later, Fang and Zhang [19] gave analytical solutions for the heat transfer over a shrinking sheet problem with a linear shrinking velocity, where both prescribed wall temperature and prescribed wall heat flux with a power-law distribution were considered.

Further, Miklavcic and Wang [20] reported the exact solution for viscous flow induced by a shrinking sheet and found non-unique solutions for certain range of suction parameter for both two-dimensional and axisymmetric cases. Later, Sajid and Hayat [21] added MHD viscous flow to this idea and solved by the homotopy analysis method (HAM) and Fang and Zhang [22] solved the full Navier-Stokes equation analytically for two-dimensional MHD viscous flow due to a shrinking sheet. Further, Sajid et al. [23] investigated the problem of MHD boundary layer flow due to a two-dimensional shrinking sheet in a rotating fluid, Hayat et al. [24] considered three-dimensional MHD and rotating flow over a porous shrinking sheet, while Lok et al. [25] studied MHD stagnation flow towards a shrinking sheet in micropolar fluid. Therefore, the aim of this study is to extend the work done by Sajid and Hayat [21] by including the energy equation with prescribed surface heat flux.

2 Problem Formulation

Consider a three-dimensional MHD viscous flow and heat transfer due to a shrinking sheet. The magnetic field with strength B_0 is applied in the $z-$ direction. In this study, we consider the electric field is zero and with the assumption that the magnetic Reynolds number is small, so that the induced magnetic field is negligible. Let (u,v,w) be the velocity components along the (x,y,z) directions, respectively. The basic governing equations of the problem are (see Miklavcic and Wang [20] and Sajid and Hayat [21])

$$\frac{\partial u}{\partial x}+\frac{\partial v}{\partial y}+\frac{\partial w}{\partial z}=0 \tag{1}$$

$$u\frac{\partial u}{\partial x}+v\frac{\partial u}{\partial y}+w\frac{\partial u}{\partial z}=-\frac{1}{\rho}\frac{\partial p}{\partial x}+\nu\left(\frac{\partial^2 u}{\partial x^2}+\frac{\partial^2 u}{\partial y^2}+\frac{\partial^2 u}{\partial z^2}\right)-\frac{\sigma B_0^2}{\rho}u \tag{2}$$

$$u\frac{\partial v}{\partial x}+v\frac{\partial v}{\partial y}+w\frac{\partial v}{\partial z}=-\frac{1}{\rho}\frac{\partial p}{\partial y}+\nu\left(\frac{\partial^2 v}{\partial x^2}+\frac{\partial^2 v}{\partial y^2}+\frac{\partial^2 v}{\partial z^2}\right)-\frac{\sigma B_0^2}{\rho}v \tag{3}$$

$$u\frac{\partial w}{\partial x}+v\frac{\partial w}{\partial y}+w\frac{\partial w}{\partial z}=-\frac{1}{\rho}\frac{\partial p}{\partial z}+\nu\left(\frac{\partial^2 w}{\partial x^2}+\frac{\partial^2 w}{\partial y^2}+\frac{\partial^2 w}{\partial z^2}\right) \tag{4}$$

$$u\frac{\partial T}{\partial x}+v\frac{\partial T}{\partial y}+w\frac{\partial T}{\partial z}=\alpha\left(\frac{\partial^2 T}{\partial x^2}+\frac{\partial^2 T}{\partial y^2}+\frac{\partial^2 T}{\partial z^2}\right) \tag{5}$$

where $\nu=\mu/\rho$ is the kinematic viscosity, σ is the electrical conductivity, ρ is the density, p is the fluid pressure, α is the thermal diffusivity and T is the fluid temperature. The boundary conditions for Eqs. (1) – (5) are

$$u=-ax,\ v=-a(m-1)y,\ w=-W,\ \frac{\partial T}{\partial z}=-\frac{q_w}{k}\ \text{at}\ y=0$$
$$u\to 0,\ T\to T_\infty\ \text{as}\ y\to\infty \tag{6}$$

where $a>0$ is the shrinking constant, k is the thermal conductivity, q_w is the surface heat flux, W is the suction velocity, $m=1$ when the sheet shrinks in $x-$direction (two-dimensional) and $m=2$ when the sheet shrinks axisymmetrically, while T_w is the sheet temperature and T_∞ is the stream temperature. Apply the following similarity transformation:

$$u=axf'(\eta),\ v=a(m-1)y\,f'(\eta),$$
$$w=-\sqrt{a\nu}\,mf(\eta),\ \eta=\sqrt{\frac{a}{\nu}}z,$$
$$\theta(\eta)=\frac{k(T-T_\infty)}{q_w}\left(\frac{a}{\nu}\right)^{1/2} \tag{7}$$

into Eqs. (1) – (5). Equation (1) is satisfied while Eq. (4) can be integrated as

$$\frac{p}{\rho}=\nu\frac{\partial w}{\partial z}-\frac{w^2}{2}+\text{constant}. \tag{8}$$

Equations (2), (3) and (5) can be reduced to

$$f''' - M^2 f' - f'^2 + m f f'' = 0 \quad (9)$$

$$\frac{1}{\Pr}\theta'' + m f \theta' = 0 \quad (10)$$

where η and θ are the independent dimensionless similarity variable and dimensionless temperature, respectively, and primes denote the differentiation with respect to η. The $f'(\eta)$ and $\theta(\eta)$ profiles refer to the velocity and temperature profiles, respectively.

The boundary conditions (6) become

$$f(0) = s,\ f'(0) = -1,\ \theta'(0) = -1,$$
$$f'(\infty) = 0,\ \theta(\infty) = 0 \quad (11)$$

where $\Pr = \nu/\alpha$ is the Prandtl number, $s = W/m\sqrt{a\nu}$ is the suction parameter and $M^2 = \sigma B_0^2/\rho a$ is the Hartmann number.

3 Numerical Procedure

Equations (9) and (10) subject to the boundary conditions (11) are solved numerically using an implicit finite-difference scheme known as the Keller-box method. The method has the following four main steps:

(i) Reduce Eqs. (9) and (10) to a first order equation;
(ii) Write the difference equations using central differences;
(iii) Linearize the resulting algebraic equations by Newton's method and write them in matrix-vector form;
(iv) Use the block-tridiagonal-elimination technique to solve the linear system, which will be discussed in detail.

3.1 The Finite-Difference Scheme

In this section, steps (i) and (ii) are combined. First, we introduce new dependent variables $u(x,\eta)$, $v(x,\eta)$, $t(x,\eta)$ and $q(x,\eta) = \theta(x,\eta)$ such that

$$f' = u,\ u' = v,\ q' = t \quad (12)$$

so that Eqs. (9) and (10) can be written as

$$v' - M^2 u - u^2 + m f v = 0 \quad (13)$$

$$t' + \Pr m f t = 0 \quad (14)$$

We now consider the net rectangle in the $x-\eta$ plane as shown in Fig. 1 and the net points defined as follows:

$$x^0 = 0,\ x^n = x^{n-1} + k_n,\quad n = 1, 2, \ldots N,$$
$$\eta_0 = 0,\ \eta_j = \eta_{j-1} + h_j,\quad j = 1, 2, \ldots J,\quad \eta_J = \eta_\infty,$$

where k_n is the Δx-spacing and h_j is the $\Delta\eta$-spacing. Here n and j are just the sequence of numbers that indicate the coordinate location, not tensor indices or exponents.

The derivatives in the x-direction are replaced by finite-difference, for example the finite-difference form for any points are

a. $$(\ )_{j-1/2}^{n} = \frac{1}{2}\left[(\ )_j^n + (\ )_{j-1}^n\right],$$
$$(\ )_j^{n-1/2} = \frac{1}{2}\left[(\ )_j^n + (\ )_j^{n-1}\right]$$

b. $$\left(\frac{\partial u}{\partial x}\right)_{j-1/2}^{n-1/2} = \frac{u_{j-1/2}^n - u_{j-1/2}^{n-1}}{k_n},$$
$$\left(\frac{\partial u}{\partial \eta}\right)_{j-1/2}^{n-1/2} = \frac{u_j^{n-1/2} - u_{j-1}^{n-1/2}}{h_j}$$

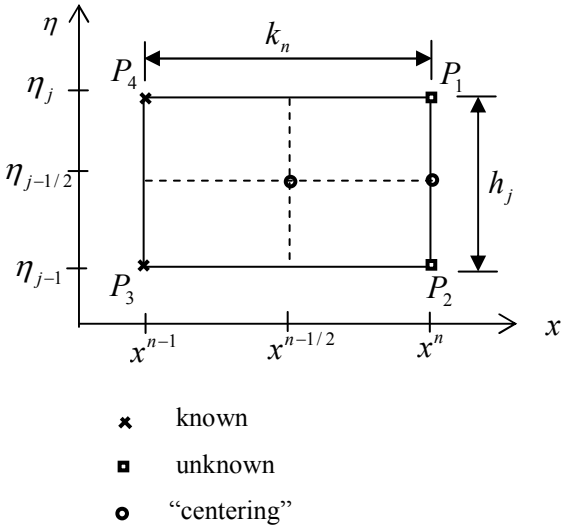

Fig. 1. Net rectangle for difference approximations

We start by writing the finite-difference form of (12) for the midpoint $\left(x^n,\eta_{j-1/2}\right)$ of the segment P_1P_2 using centered-difference derivatives. This process is called "centering about $\left(x^n,\eta_{j-1/2}\right)$". We get

$$\begin{aligned}
&f_j - f_{j-1} - \frac{1}{2}h_j\left(u_j + u_{j-1}\right) = 0\\
&u_j - u_{j-1} - \frac{1}{2}h_j\left(v_j + v_{j-1}\right) = 0\\
&q_j - q_{j-1} - \frac{1}{2}h_j\left(t_j + t_{j-1}\right) = 0\\
&\left(v_j - v_{j-1}\right) - M^2\frac{h_j}{2}\left(u_j + u_{j-1}\right) - \frac{h_j}{4}\left(u_j + u_{j-1}\right)^2\\
&\qquad + m\frac{h_j}{4}\left(f_j + f_{j-1}\right)\left(v_j + v_{j-1}\right) = 0\\
&\left(t_j - t_{j-1}\right) + \frac{h_j}{4}(\mathrm{Pr})m\left(f_j + f_{j-1}\right)\left(t_j + t_{j-1}\right) = 0
\end{aligned} \tag{15}$$

Equations (15) are imposed for j = 1, 2… J at given n, and the transformed boundary layer thickness, η_J, is to be sufficiently large so that it is beyond the edge of the boundary layer, see Keller and Cebeci [26]. The boundary conditions yield at $x = x^n$ are

$$f_0^n = s\,,\ u_0^n = -1\,,\ t_0^n = -1\,,\ u_J^n = 0\,,\ q_J^n = 0\,. \tag{16}$$

3.2 Newton's Method

For simplicity, the unknown parameters $\left(f_j^n, u_j^n, v_j^n\right)$ at $x = x^n$ is written by $\left(f_j, u_j, v_j\right)$. To linearize the nonlinear system of equations (15) using Newton's method, we introduce the following iterates:

$$\begin{aligned}
&f_j^{(i+1)} = f_j^{(i)} + \delta f_j^{(i)}, u_j^{(i+1)} = u_j^{(i)} + \delta u_j^{(i)},\\
&v_j^{(i+1)} = v_j^{(i)} + \delta v_j^{(i)}\,,\ q_j^{(i+1)} = q_j^{(i)} + \delta q_j^{(i)}\,,\\
&t_j^{(i+1)} = t_j^{(i)} + \delta t_j^{(i)}\,.
\end{aligned} \tag{17}$$

Substituting these expressions into (15), then drop the quadratic and higher-order terms in $\delta f_j^{(i)}$, $\delta u_j^{(i)}$, $\delta v_j^{(i)}$, $\delta q_j^{(i)}$, $\delta t_j^{(i)}$, this procedure yields the following linear tridiagonal system:

$$\delta f_j - \delta f_{j-1} - \frac{1}{2}h_j\left(\delta u_j + \delta u_{j-1}\right) = \left(r_1\right)_{j-1/2},$$

$$\delta u_j - \delta u_{j-1} - \frac{1}{2}h_j\left(\delta v_j + \delta v_{j-1}\right) = \left(r_2\right)_{j-1/2},$$

$$\delta q_j - \delta q_{j-1} - \frac{1}{2}h_j\left(\delta t_j + \delta t_{j-1}\right) = \left(r_3\right)_{j-1/2}, \tag{18}$$

$$\begin{aligned}
&\left(a_1\right)_j \delta v_j + \left(a_2\right)_j \delta v_{j-1} + \left(a_3\right)_j \delta f_j +\\
&\left(a_4\right)_j \delta f_{j-1} + \left(a_5\right)_j \delta u_j + \left(a_6\right)_j \delta u_{j-1} = \left(r_4\right)_{j-1/2}\\
&\left(b_1\right)_j \delta t_j + \left(b_2\right)_j \delta t_{j-1} + \left(b_3\right)_j \delta f_j +\\
&\qquad\qquad \left(b_4\right)_j \delta t_{j-1} = \left(r_5\right)_{j-1/2}
\end{aligned}$$

where

$$\begin{aligned}
&\left(a_1\right)_j = 1 + \frac{1}{2}h_j m f_{j-1/2}, \left(a_2\right)_j = \left(a_1\right)_j - 2,\\
&\left(a_3\right)_j = \frac{1}{2}h_j m v_{j-1/2}, \left(a_4\right)_j = \left(a_3\right)_j,\\
&\left(a_5\right)_j = -\frac{1}{2}h_j M^2 - h_j u_{j-1/2}, \left(a_6\right)_j = \left(a_5\right)_j,\\
&\left(b_1\right)_j = 1 + \frac{1}{2}h_j m\,\mathrm{Pr}\, f_{j-1/2}, \left(b_2\right)_j = \left(b_1\right)_j - 2,\\
&\left(b_3\right)_j = \frac{1}{2}h_j\,\mathrm{Pr}\, t_{j-1/2}, \left(b_4\right)_j = \left(b_3\right)_j
\end{aligned} \tag{19}$$

and

$$\begin{aligned}
&\left(r_1\right)_{j-1/2} = f_{j-1} - f_j + h_j u_{j-1/2},\\
&\left(r_2\right)_{j-1/2} = u_{j-1} - u_j + h_j v_{j-1/2},\\
&\left(r_3\right)_{j-1/2} = q_{j-1} - q_j + h_j t_{j-1/2},\\
&\left(r_4\right)_{j-1/2} = \left(v_{j-1} - v_j\right) + h_j M^2 u_{j-1/2} + h_j u_{j-1/2}^2 -\\
&\qquad h_j m\left(f_{j-1/2} v_{j-1/2}\right)\\
&\left(r_5\right)_{j-1/2} = \left(t_{j-1} - t_j\right) - h_j m\,\mathrm{Pr}\left(f_{j-1/2} t_{j-1/2}\right)
\end{aligned} \tag{20}$$

To complete the system (18) we use the boundary conditions (16), which can be satisfied exactly with no iteration. Therefore, in order to maintain these correct values in all the iterates, we take

$$\delta f_0 = 0,\ \delta u_0 = 0,\ \delta t_0 = 0,\ \delta u_J = 0,\ \delta q_J = 0. \tag{21}$$

3.3 The Block Tridiagonal Matrix

The linearized difference system (18) has a block tridiagonal structure consists of variables or constants, but here it consists of block matrices. The elements of the matrices are defined as follows:

$$\begin{bmatrix} [A_1] & [C_1] & & & & \\ [B_2] & [A_2] & [C_2] & & & \\ & \ddots & \ddots & & & \\ & & \ddots & & & \\ & & & [B_{J-1}] & [A_{J-1}] & [C_{J-1}] \\ & & & & [B_J] & [A_J] \end{bmatrix} \begin{bmatrix} [\delta_1] \\ [\delta_2] \\ \vdots \\ [\delta_{J-1}] \\ [\delta_J] \end{bmatrix}$$

$$= \begin{bmatrix} [r_1] \\ [r_2] \\ \vdots \\ [r_{J-1}] \\ [r_J] \end{bmatrix}$$

That is :

$$\mathbf{A\delta = r} \tag{22}$$

where

$$[A_1] = \begin{bmatrix} 0 & 0 & 1 & 0 & 0 \\ d & 0 & 0 & d & 0 \\ 0 & -1 & 0 & 0 & d \\ (a_2)_j & 0 & (a_3)_j & (a_1)_j & 0 \\ 0 & 0 & (b_3)_j & 0 & (b_1)_j \end{bmatrix}, \tag{23}$$

$$[A_j] = \begin{bmatrix} d & 0 & 1 & 0 & 0 \\ -1 & 0 & 0 & d & 0 \\ 0 & -1 & 0 & 0 & d \\ (a_6)_j & 0 & (a_3)_j & (a_1)_j & 0 \\ 0 & 0 & (b_3)_j & 0 & (b_1)_j \end{bmatrix}, 2 \le j \le J \tag{24}$$

$$[B_j] = \begin{bmatrix} 0 & 0 & -1 & 0 & 0 \\ 0 & 0 & 0 & d & 0 \\ 0 & 0 & 0 & 0 & d \\ 0 & 0 & (a_4)_j & (a_2)_j & 0 \\ 0 & 0 & (b_4)_j & 0 & (b_2)_j \end{bmatrix}, 2 \le j \le J \tag{25}$$

$$[Cj] = \begin{bmatrix} d & 0 & 0 & 0 & 0 \\ 1 & 0 & 0 & 0 & 0 \\ 0 & 1 & 0 & 0 & 0 \\ (a_5)_j & 0 & 0 & 0 & 0 \\ 0 & 0 & 0 & 0 & 0 \end{bmatrix}, 1 \le j \le J-1 \tag{26}$$

where $d = -\dfrac{h_j}{2}$,

$$[\delta_1] = \begin{bmatrix} \delta v_0 \\ \delta q_0 \\ \delta f_1 \\ \delta v_1 \\ \delta t_1 \end{bmatrix}, \quad [\delta_j] = \begin{bmatrix} \delta u_{j-1} \\ \delta q_{j-1} \\ \delta f_j \\ \delta v_j \\ \delta t_j \end{bmatrix}, \quad 2 \le j \le J \tag{27}$$

$$\text{and } [r_j] = \begin{bmatrix} (r_1)_{j-1/2} \\ (r_2)_{j-1/2} \\ (r_3)_{j-1/2} \\ (r_4)_{j-1/2} \\ (r_5)_{j-1/2} \end{bmatrix}, \quad 1 \le j \le J. \tag{28}$$

To solve Eq. (22), we assume that matrix **A** is nonsingular and it can be factored into

$$\mathbf{A = LU} \tag{29}$$

where

$$\mathbf{L} = \begin{bmatrix} [\alpha_1] & & & & \\ [B_2] & [\alpha_2] & & & \\ & \ddots & & & \\ & \ddots & [\alpha_{J-1}] & & \\ & & [B_J] & [\alpha_J] \end{bmatrix} \text{ and}$$

$$\mathbf{U} = \begin{bmatrix} [I] & [\Gamma_1] & & & & \\ & [I] & [\Gamma_2] & & & \\ & & \ddots & & & \\ & & \ddots & & & \\ & & & & [I] & [\Gamma_{J-1}] \\ & & & & & [I] \end{bmatrix}$$

where [*I*] is the identity matrix of order 5 and $[\alpha_i]$, and $[\Gamma_i]$ are 5×5 matrices which elements are determined by the following equations:

$$[\alpha_1] = [A_1], \tag{30}$$

$$[A_1][\Gamma_1] = [C_1], \tag{31}$$

$$[\alpha_j] = [A_j] - [B_j][\Gamma_{j-1}], \; j = 2, 3, \ldots, J \tag{32}$$

$$[\alpha_j][\Gamma_j] = [C_j], \; j = 2, 3, \ldots, J\text{-}1. \tag{33}$$

Equation (29) can now be substituted into Eq. (22), and we get

$$\mathbf{LU\delta} = \mathbf{r}. \quad (34)$$

If we define $\mathbf{U\delta} = \mathbf{W}$, (35)

then Eq. (34) becomes $\mathbf{LW} = \mathbf{r}$, (36)

where

$$\mathbf{W} = \begin{bmatrix} [W_1] \\ [W_2] \\ \vdots \\ [W_{J-1}] \\ [W_J] \end{bmatrix}$$

and the $[W_j]$ are 5 × 1 column matrices. The elements $\mathbf{W}$ can be solved from Eq. (36)

$$[\alpha_1][W_1] = [r_1], \quad (37)$$

$$[\alpha_j][W_j] = [r_j] - [B_j][W_{j-1}],\ 2 \le j \le J. \quad (38)$$

The step in which Γ_j, α_j and W_j are calculated is usually referred to as the forward sweep. Once the elements of $\mathbf{W}$ are found, Eq. (35) then gives the solution δ in the so-called backward sweep, in which the elements are obtained by the following relations:

$$[\delta_J] = [W_J], \quad (39)$$

$$[\delta_j] = [W_j] - [\Gamma_j][\delta_{j+1}],\ 1 \le j \le J-1. \quad (40)$$

These calculations are repeated until some convergence criterion is satisfied and calculations are stopped when

$$\left|\delta v_0^{(i)}\right| < \varepsilon_1 \quad (41)$$

where ε_1 is a small prescribed value.

4 Results and Discussion

Equations (9) and (10) subject to the boundary conditions (11) are solved numerically using the implicit finite-difference scheme known as the Keller-box method as described in the books by Na [27], Cebeci and Bradshaw [28] and Cebeci and Cousteix [29]. The Keller-box method is programmed in MATLAB with the step size of $\Delta\eta$ = 0.01 in η and then solved for the interval of $0 \le \eta \le \eta_\infty$, where η_∞ is the boundary layer thickness or the edge of boundary layer. A solution is considered to converge when the difference between the input and the output values of $v(x,0)$ are within 0.00001 or 1×10^{-5}.

For the validation of the numerical method used in this study, the case of $M^2 = 4$ and $s = 1$ are compared with those of Sajid and Hayat [21]. The numerical values for the skin friction coefficient are $f''(0) = 2.3028$ for $m = 1$, and $f''(0) = 2.8916$ for $m = 2$, while Sajid and Hayat [21] reported the values $f''(0) = 2.30277$ for $m = 1$, and $f''(0) = 2.89160$ for $m = 2$. The comparison is found to be very good.

The effects of suction parameter on velocity and temperature profiles are shown in Figs. 2 and 3. When the value of *s* increases the velocity profiles also increase and become closer to the surface and the tangential velocity becomes steeper, hence the skin friction coefficient (first solution) $f''(0)$ increases, while the wall temperature $\theta(0)$ (first solution) is found to decrease with *s*, as shown in Table 1 (for $m = 1$) and Table 2 (for $m = 2$). Table 1 also shows the existence of the dual solutions of the problem for non-zero magnetic field, namely $M^2 = 0.25$. Figure 3 shows the temperature profiles decrease and also become closer to the surface, as the value of *s* increases.

Table 1. Values of $f''(0)$ and $\theta(0)$ for various *s* when $m = 1$, Pr = 0.7 and M^2 = 0.25

s	$f_1''(0)$	$f_2''(0)$	$\theta_1(0)$	$\theta_2(0)$
1.75	1.0000	0.7550	1.2313	1.5031
1.80	1.1449	0.6551	1.1109	1.6475
1.85	1.2500	0.6000	1.0356	1.8268
1.90	1.3405	0.5595	0.9776	2.0808

Table 2. Values of $f''(0)$ and $\theta(0)$ for various *s* when $m = 2$, Pr = 0.7 and M^2 = 5

s	2.0	2.3	3.0	3.5
$f''(0)$	4.7461	5.2705	6.5387	7.4708
$\theta(0)$	0.3835	0.3278	0.2459	0.2090

Table 3. Values of $\theta(0)$ for various Pr, $M^2 = 5$ and $s = 3$

Pr	$m = 1$	$m = 2$
0.7	0.5044	0.2459
1	0.3505	0.1713
3	0.1142	0.0563
7	0.0484	0.0240
10	0.0337	0.0168
15	0.0224	0.0112
20	0.0168	0.0084
30	0.0112	0.0056

The effect of Hartmann number M^2 on velocity and temperature profiles can be seen from Figs. 4 and 5. It is shown that the velocity profiles also increase with Hartmann number and from Fig.5, for both cases, $m = 1$ and $m = 2$, the temperature profiles show that the profiles are not affected much by the increment in M^2. Figure 6 illustrates that as Pr increases, this leads to the decrease of the temperature profiles and the thermal boundary layer thickness becomes smaller. This phenomenon occurs because when Pr increases, the thermal diffusivity decreases, thus it leads to the decrease of the energy transfer ability that decreases the thermal boundary layer. Therefore, as Pr increases, the wall temperature decreases for both $m = 1$ and $m = 2$, as shown in Table 2. It is worth mentioning that small values of Pr (<< 1) physically correspond to liquid metals, $\Pr \sim 1$ corresponds to diatomic gases including air and large values of Pr (>> 1) correspond to high-viscosity oils and $\Pr \sim 7$ corresponds to water at room temperature.

The velocity and temperature profiles of the second solutions are displayed in Figs. 7 and 8. These profiles prove that the dual solutions exist for a certain range of suction parameter for non-zero Hartmann number when the sheet shrinks in two-dimensional way. Figures 9 and 10 display the skin friction coefficient and the reciprocal of wall temperature for various s and M^2. Dual solutions are found to exist only for $0 \le M^2 < 1$. The dual solution for full Navier-Stokes equation can be found in [22]. Unique solution is obtained for $M^2 \ge 1$. Further, results for $s < s_c$ are unable to be obtain due to the boundary layer approximation breaks down at $s = s_c$, therefore, the boundary layer has separated from the surface. The boundary layer started to separate from the surface at $s = s_c$ where $s_c = 2$ for $M^2 = 0$ (zero Hartmann number) and $s_c = 1.735$ for $M^2 = 0.25$. Hence, boundary layer separation delayed with Hartmann number.

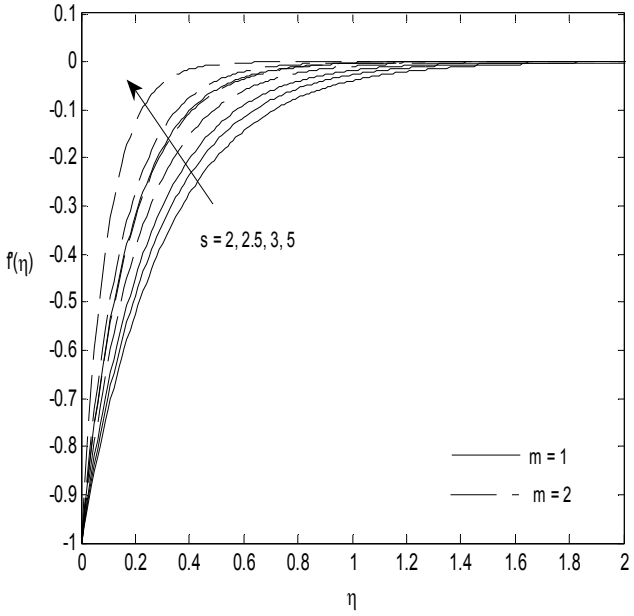

Fig. 2. Velocity profiles for various s when $M^2 = 5$, Pr = 0.7

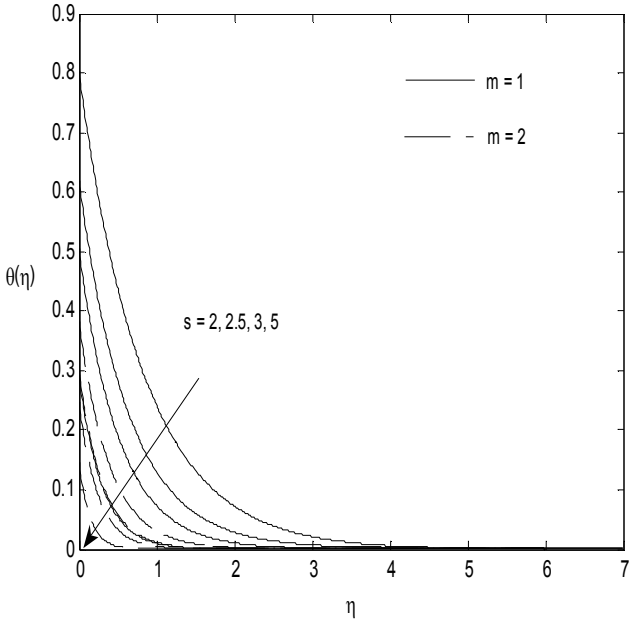

Fig. 3. Temperature profiles for various s when $M^2 = 5$, Pr = 0.7

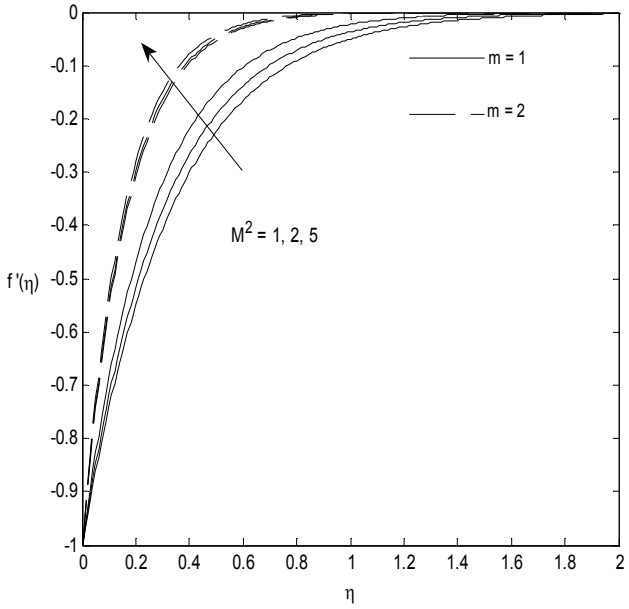

Fig. 4. Velocity profiles for various M^2 when $s = 3$, Pr = 0.7

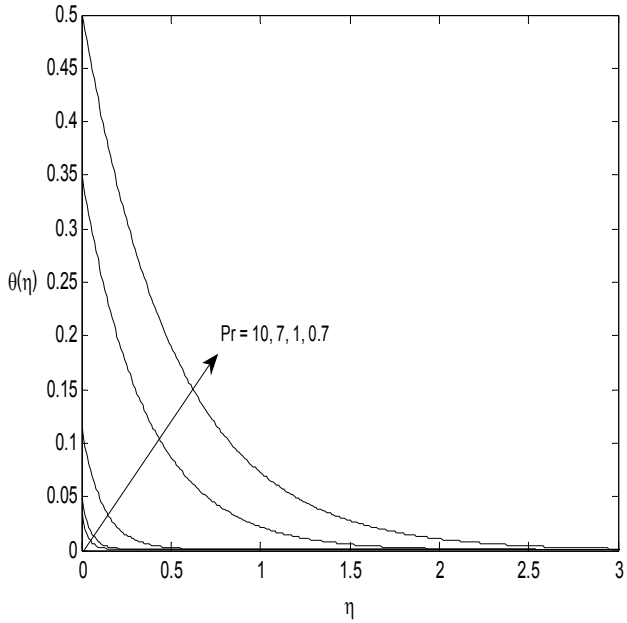

Fig. 6. Temperature profiles for various Pr when $M^2 = 5$, $s = 3$

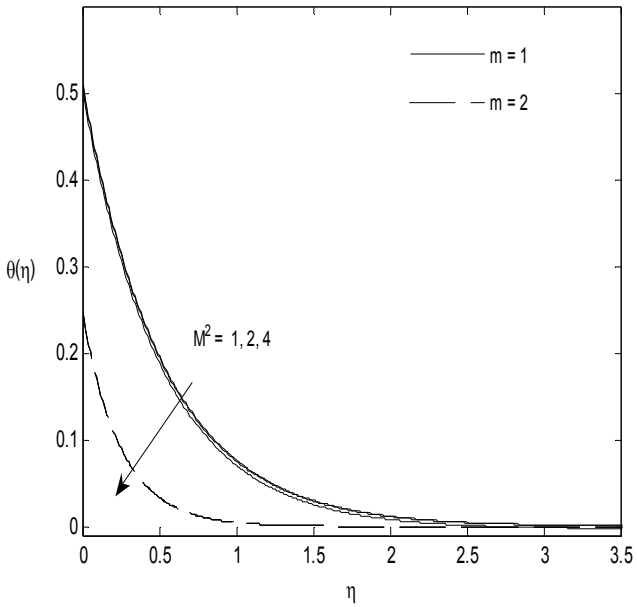

Fig. 5. Temperature profiles for various M^2 when $s = 3$, Pr = 0.7

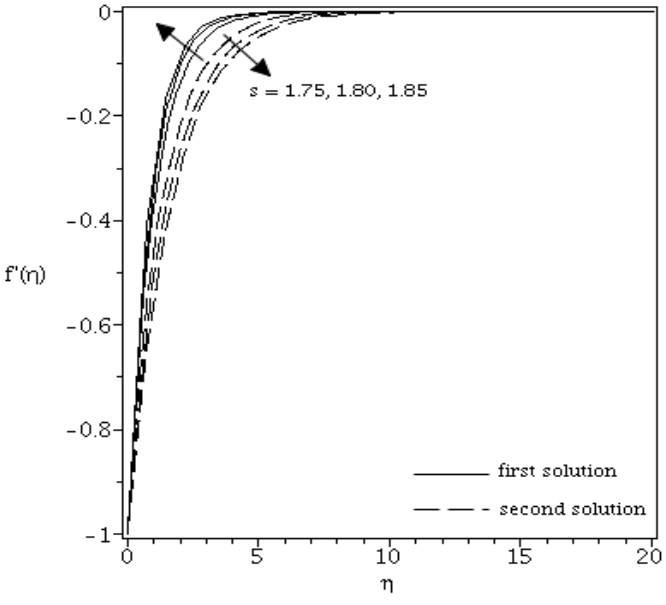

Fig. 7. Velocity profiles for various s when Pr = 0.7, $M^2 = 0.25$

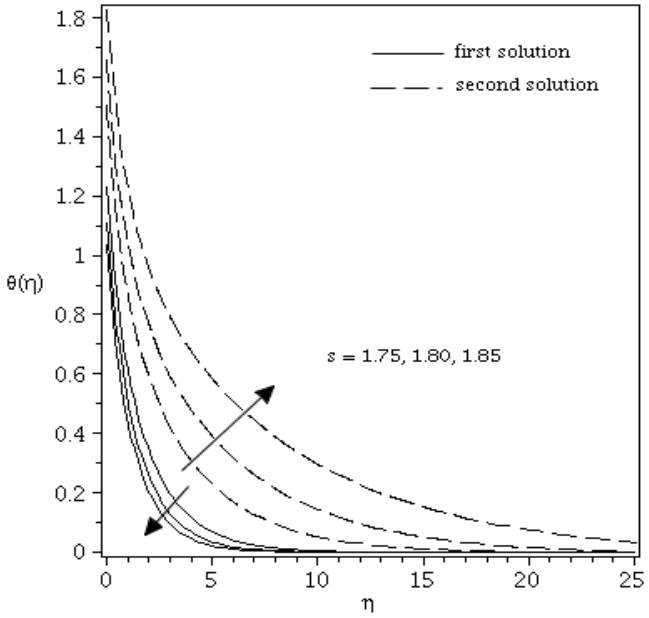

Fig. 8. Temperature profiles for various s when Pr = 0.7, $M^2 = 0.25$

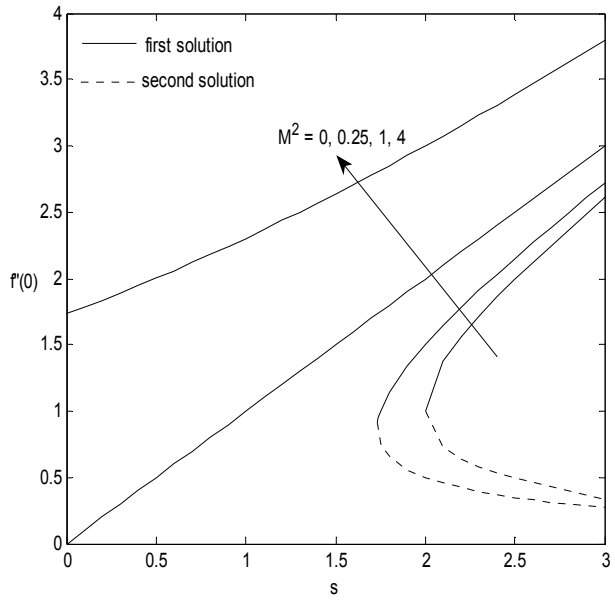

Fig. 9. Variation of the skin friction coefficient $f''(0)$ with s for various M^2 when Pr = 0.7

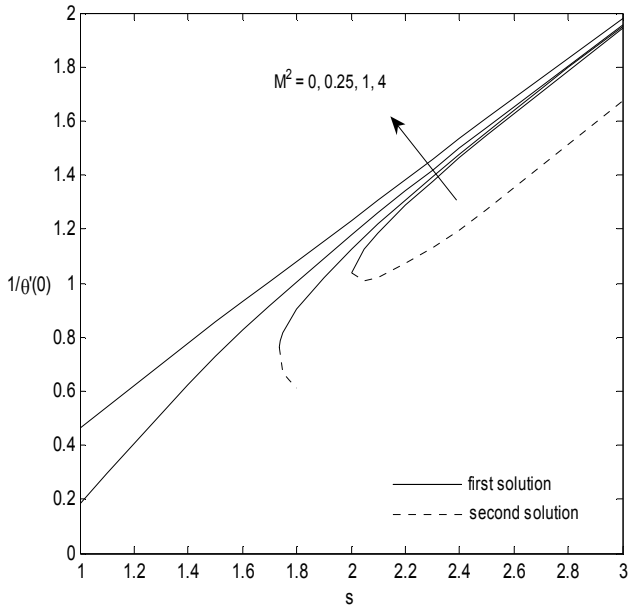

Fig. 10 Variation of the $1/\theta(0)$ with s for various M^2 when Pr = 0.7

5 Conclusions

A numerical study was performed for the problem of MHD viscous flow and heat transfer due to a permeable shrinking sheet with prescribed surface heat flux. The skin friction coefficient was found to increase with the increase of the suction parameter, while the wall temperature shows opposite trend. The thermal boundary layer thicknesses as well as the temperature profiles reduce with suction parameter and Prandtl number. In this study, the temperature profiles are most affected by the suction parameter and the Prandtl number. Dual solutions are also obtained for certain range of the suction parameter when the sheet shrinks in two-dimensional for non-zero Hartmann number. In this study, it is also found that the Hartmann number delayed the separation of the boundary layer. The velocity boundary layer thickness and the thermal boundary layer thickness for the axisymmetrically case are always smaller than the two-dimensional case.

Acknowledgements

The authors gratefully acknowledge the financial supports received from the Universiti Putra Malaysia (Research University Grant Scheme, RUGS) and the research university grant (GUP) from the Universiti Kebangsaan Malaysia.

References:

[1] H. Blasius, Grenzschichten in Flüssigkeiten mit kleiner Reibung, *Zeitschrift für Mathematik Physik*, Vol.56, 1908, pp.1-37.

[2] BC. Sakiadis, Boundary layer behavior on continuous solid surfaces. II. Boundary layer on a continuous flat surface, *AIChEJ*, Vol. 7, 1961, pp. 221-225.

[3] LJ. Crane, Flow past a stretching plate, *Journal of Applied Mathematics and Physics (ZAMP)*, Vol. 21, 1970, pp. 645-647.

[4] PS. Gupta, AS. Gupta, Heat and mass transfer on a stretching sheet with suction and blowing, *Canadian Journal of Chemical Engineering*, Vol. 55, 1977, pp. 744-746.

[5] E. Magyari, B. Keller, B, Exact solutions for self-similar boundary-layer flows induced by permeable stretching walls, *European Journal of Mechanics B-Fluids*, Vol. 19, 2000, pp. 109--122

[6] CY. Cheng, Magnetic field effects on coupled heat and mass transfer by mixed convection along a vertical surface embedded in a porous medium by integral methods, *Proceedings of the 4th WSEAS International Conference on Heat and Mass Transfer*, Gold Coast, Queensland, Australia, January, 2007, pp. 86-91.

[7] T. Al-Azab, Unsteady mixed convection heat and mass transfer past an infinite porous plate with thermophoresis effect, *WSEAS Transactions on Heat and Mass Transfer*, Vol. 4, Issue 2, 2009, pp. 23-33.

[8] Z. Boricic, D. Nikodijevic, B. Blagojevic, Z. Stamenkovic, Universal solutions of unsteady two-dimensional MHD boundary layer on the body with temperature gradient along surface, *WSEAS Transactions on Fluid Mechanics*, Vol. 4, Issue 3, 2009, pp. 97-106.

[9] M. Narahari, Natural convection of unsteady Couette flow between two vertical parallel plates in the presence of constant heat flux and radiation, *Proceedings of the 11th WSEAS International Conference on Mathematical and Computational Methods in Science and Engineering*, Morgan State University, Baltimore, USA, November, 2009, pp. 73-78.

[10]JH. Merkin, T. Mahmood, Mixed convection boundary layer similarity solutions: prescribed wall heat flux, *Journal of Applied Mathematics and Physics (ZAMP)*, Vol. 40, 1989, pp. 51-68.

[11]N. Ramachandran, TS. Chen, BF. Armaly, Mixed convection in stagnation flows adjacent to vertical surfaces, *Journal of Heat Transfer*, Vol. 110, 1988, pp. 373-377.

[12]A. Ishak, Mixed convection boundary layer flow over a vertical cylinder with prescribed surface heat flux, *Journal of Physics A: Mathematical and Theoretical*, Vol. 42, 2009, pp. 195501.

[13]N. Bachok, A. Ishak, The effects of suction and injection on a moving flat plate in a parallel stream with prescribed surface heat flux, *Proceedings of the 9th WSEAS International Conference on Applications of Computer Engineering*, Penang, Malaysia, March, 2010, pp. 111-118.

[14]T. Fang, Boundary layer flow over a shrinking sheet with power-law velocity, *International Journal of Heat and Mass Transfer*, Vol. 51, 2008, pp. 5838-5843.

[15]CY. Wang, Stagnation flow towards a shrinking sheet, *International Journal of Non-Linear Mechanics*, Vol. 43, 2008, pp. 377-382.

[16]M. Rahimpour, SR. Mohebpour, A. Kimiaeifar, GH. Bagheri, On the analytical solution of axisymmetric stagnation flow towards a shrinking sheet, *International Journal of Mechanics*, Vol. 2, No. 1, 2008, pp. 1-10.

[17]TG. Fang, J. Zhang J, S-S Yao, Viscous flow over an unsteady shrinking sheet with mass transfer, *Chinese Physics Letters*, Vol. 26, 2009, pp. 014703-1-014703-4.

[18]FM. Ali, R. Nazar, NM. Arifin, I. Pop, Unsteady shrinking sheet with mass transfer in a rotating fluid, *International Journal for Numerical Methods in Fluids*, DOI: 10.1002/fld.2325, 2010 (in press)

[19]TG. Fang, J. Zhang, Thermal boundary layers over a shrinking sheet: an analytical solution, Acta Mechanica, Vol. 209, 2010, pp. 325-343.

[20]M. Miklavcic, CY. Wang, Viscous flow due to a shrinking sheet, *Quarterly of Applied Mathematics*, Vol. 64, 2006, pp. 283-290.

[21]M. Sajid, T. Hayat, The application of homotopy analysis method for MHD viscous flow due to a shrinking sheet, *Chaos, Solitons and Fractals*, Vol. 39, 2009, pp. 1317-1323.

[22]T. Fang, J. Zhang , Closed-form exact solutions of MHD viscous flow over a shrinking sheet, *Communication in Nonlinear Science and Numerical Simulation*, Vol. 14, 2009, pp. 2853-2857.

[23]M. Sajid, T. Javed, T. Hayat, MHD rotating flow of a viscous fluid over a shrinking surface. *Nonlinear Dynamic*, Vol. 51, 2008, pp. 259-265.

[24]T. Hayat, Z. Abbas, T. Javed, M. Sajid, Three-dimensional rotating flow induced by a shrinking sheet for suction. *Chaos, Solitons and Fractals*, Vol. 39, 2009, pp. 1615-1626.

[25]YY. Lok, A. Ishak, I. Pop, MHD stagnation-point flow towards a shrinking sheet,

International Journal for Numerical Methods in Heat Fluid Flow, 2009, online.

[26]HB. Keller, T. Cebeci, Accurate numerical methods for boundary layer flows. II: Two-dimensional turbulent flows, *AIAA Journal*, vol. 10, 1972, pp. 1193-1199.

[27]TY. Na, *Computational Methods in Engineering Boundary Value Problem*, Academic Press, 1979.

[28]T. Cebeci, P. Bradshaw, *Physical and Computational Aspects of Convective Heat Transfer*, Springer, 1984.

[29]T. Cebeci, J. Cousteix, *Modeling and Computing of Boundary-Layer Flows: Laminar, Turbulent and Transitional Boundary Layers in Incompressible and Compressible Flows*, Springer, 2005.